Original Research Article

A Hydrodynamic Model of Flow in a Bifurcating Stream, Part 1: Effects of Bifurcation Angle and Magnetic Field

Abstract A hydrodynamic model of the flow in a bifurcating stream is presented. The problem is modeled using the Boussinesq approximations, and the governing nonlinear equations solved analytically by the methods of similarity transformation and regular perturbation series expansions. Similarity expressions for the temperature, concentration and velocity are obtained and analyzed graphically. The results show that bifurcation angle and Reynolds number increase the transport velocity. Furthermore, it is seen that the magnetic field parameter decreases the velocity in the upstream region, and makes it oscillatory in the downstream region.

Keywords: bifurcation, hydrodynamic model, magnetic field, porous, perturbation method, similarity transformation, stream

NOMENCLATURE

C' concentration (quantity of material being transported)
D diffusion coefficient
g gravitational field vector
Gc Grashof number due to concentration difference
Gr Grashof number due to temperature difference
p' fluid pressure
p dimensionless pressure
Pr Prandtl number
Q heat absorption coefficient
Re Reynolds number,
Sc Schmidt number
T' fluid temperature
(u', v') velocity components of the fluid in the mutually orthogonal axes
(u, v) non-dimensionalized velocity components
(x', y') mutually orthogonal axes
(x, y) dimensionless orthogonal axes
α , β bifurcation angles
ρ' density of the fluid
ρ dimensionless density of the fluid
μ viscosity of the fluid
μ_m magnetic permeability of the fluid
κ permeability of the porous medium
σ_e electrical conductivity of the fluid
υ kinematic viscosity of the fluid
χ^2 local Darcy number
δ_1^2 rate of chemical reaction
Θ dimensionless temperature
Φ dimensionless concentration
B_c volumetric expansion coefficient due to concentration

B_o^2 applied uniform magnetic field strength

B_t volumetric expansion coefficient due to temperature

C_p specific heat capacity at constant pressure

C_w constant wall temperature maintained

C_∞ concentration at equilibrium

k_o thermal conductivity of the medium

k_r^2 rate of chemical reaction

ℓ_c scale length

M^2 Hartmann's number

N^2 heat exchange parameter

p_∞ ambient/equilibrium pressure

T_w constant wall concentration at which the channel is maintained

T_∞ temperature at equilibrium

U_o characteristic velocity of the flow

1 INTRODUCTION

The strength of a stream depends on its mass-volume and velocity. And its velocity, amongst others, depends on the difference in gradient between its source in the mountain and mouth in a standing water body ([1], [2]). Based on the slope differential, a stream can be divided into three regions: the erosion (upper or torrent) zone; the transfer (middle or valley) zone, and the depositional zone. In the erosion zone, the stream flows through a deep descent; therefore, its velocity is very high and the flow very erosive. Here, the flow vertically down-cuts and removes the bed rocks from the valley floor and sides. In the mid-valley course, the gradient is lower than that of the upper course and so is the velocity, but it is able to carry the eroded materials and rocks farther. In the depositional course, the gradient is very low and so is the flow such that the rate of deposition of materials on the stream bed, and on the flood plain during flood is very high.

Several features like the braided streams (or rivers), anastomosing stream, meanders and the likes are formed in the depositional zone ([1], [2]). In particular, anastomosing rivers represent a type of rivers that are currently of interest in geomorphology and sedimentology. They have multiple inter-connected channels separated by areas of the flood plains. Usually, in the tropical region, the river banks are stabilized by vegetation and in the arid region by highly consolidated rocks. They help to inhibit lateral migration of channels. However, at points where the banks have loose structures, the stream may suddenly abandon its old course for a new course or part of its old course to form a by-pass. At the points of the by-pass, the river is said to divide or anastomose ([1], [2]).

Much of the works on stream flow have been carried out using non-hydrodynamic approaches. Some used the hydrologic model, which involves the use of spatial form of continuity equation or water balance and flux relation expressing storage as a function of inflow and outflow (see [3]); some the hydraulic model, which is based on the use of St. Venant equations (see [4]), and others the stochastic probability model, which involves the use of Monte Carlo method (see [5], [6]). All these used computer simulation techniques. Therefore, we are motivated to study the flow hydrodynamically and analytically. Thus, this study intends to develop a hydrodynamic model of the flow in a bifurcating stream.

Some reports exist in literature on flow in both bifurcating and non-bifurcating channels. For example, [7], [8], [9], [10], [12] and [13] examined numerically and experimentally the flow structure in bifurcating systems and observed that bifurcation angle increases the inlet pressure and subsequently increases the

flow velocity of such systems. Similarly, [14, 15] studied the magneto-hydrodynamic viscous steady bio-fluid flow through a curved pipe with circular cross-section under various conditions, using spectral method as the principal tool and the Fourier series, Chebyshev polynomials, collocation and iteration methods as secondary tools, and observed that the axial velocity increases with an increase in the Dean number, whereas it is suppressed with greater curvature and magnetic field parameter. Moreso, [16] examined the magneto-hydrodynamic laminar blood flow through a curved blood vessel with circular cross-section, using spectral collocation algorithm, and noticed that the axial velocity is displaced towards the centre of the vessel with corresponding low fluid particle vortices for high magnetic field parameter, Dean number and low curvature; [17] investigated the combined effects of rotation (coriolis force), magnetic field and curvature (centrifugal force) on the steady flow of an incompressible viscous fluid through a rotating curved pipe of circular cross-section and magnetic field using spectral method of solution, and observed that for a high magnetic field, four-vortex solution is seen in rotating curved systems. Most recently, [18] studied the flow of blood in convergent and divergent channels using the method of perturbation series expansion, and noticed that Reynolds number increases the flow velocity.

Apart from the gradient differential, a number of factors affect the flow of a stream, dynamically. Based on this, the purpose of this paper is to investigate the effects of bifurcation angles and the nature of the source rocks on the flow of a bifurcating stream.

This paper is organized in the following manner: section 2 is the methodology; section 3 holds the results and discussion, and section 4 gives the conclusions.

2 METHODOLOGY

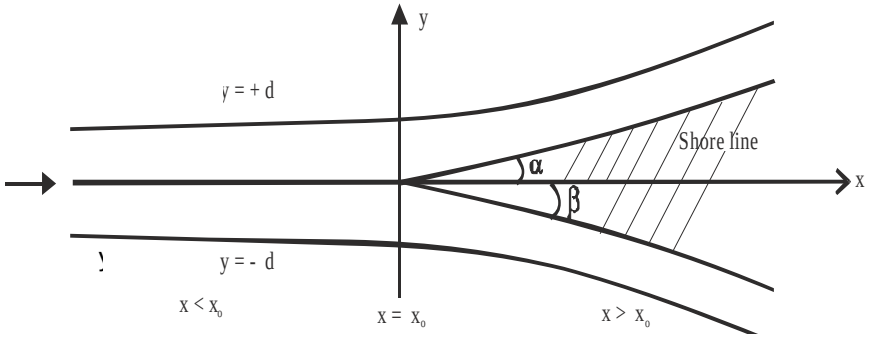

Figure 1 A physical model of symmetrical bifurcating flowing stream (α=β).

The stream is approximately rectangular in form and planar at the surface. We assume that the flow is axi-symmetrical about the z'-axis; the fluid is incompressible, Newtonian, magnetically susceptible (due to the nature of the source rock), chemically reacting, and of a homogeneous first order type (i.e. the reaction is proportional to the concentration); the fluid viscosity is a function of temperature and magnetic field; the porous medium is non-homogeneous, therefore, its permeability is anisotropic; the fluid have constant properties except that the density varies with the temperature and concentration which are considered only in the force term. If (u', v') are respectively the velocity components of the fluid in the mutually orthogonal (x', y') axes, the mathematical equations of mass balance/continuity, momentum, energy and diffusion governing the flow in the presence of bifurcation, and considering the Boussinesq and Swell's free flow in vector form become:

$$\nabla . v' = 0 \tag{1}$$

$$(v'.\nabla)v' = \frac{-1}{\rho'}\nabla p' + \frac{\mu}{\rho'}\nabla^2 v' + g\beta_t(T' - T_\infty) + g\beta_c(C' - C_\infty - \frac{\mu}{\rho'\kappa}v' - \frac{\sigma_e B^2{}_o v'}{\rho'^2 \mu\mu_m} \tag{2}$$

$$(v'.\nabla)T' = \frac{k_o}{\rho' C_p}\nabla^2 T' + \frac{Q}{\rho' C_p}(T' - T_\infty) \tag{3}$$

$$\left(v'.\nabla\right)C' = D\nabla^2 C' + k^2{}_r\left(C' - C_\infty\right) \tag{4}$$

The problem examines the dynamics of a bifurcating stream flowing from a point $x' = -\infty$ towards a shore at $x' = x_o$, as seen in Figure 1. The model shows that the channel is assumed to be symmetrical and divided into two regions: the upstream (or mother) region $x' < x_o$ and downstream (or daughter) region $x' > x_o$, where x_o is the bifurcation or the nodal point, which is assumed to be the origin such that the stream boundaries become $y' = \pm d$ for the upstream region and $y' = \alpha x'$ for the downstream region. Due to geometrical transition between the mother and daughter channels, the problem of wall curvature effect is bound to occur. To fix up this, a very simple transition wherein the width of the daughter channel is made equal to half that of the mother channel i.e. $\pm d$ such that the variation of the bifurcation angle is straight-forwardly used (see [13]). Furthermore, if the width of the stream ($2d$) is far less than its length (l_o) before the point of bifurcation such that the ratio of $\frac{2d}{l_o} = \Re << 1$, (where $\Re$ is the aspect ratio), the flow is laminar and Poiseuille (see [19]). d is assumed to be non-dimensionally equal to one (see [14]). Similarly, at the entry region of the mother channel, the flow velocity is given as $u' = U_o\left(1 - y'^2\right)$, where U_o is the characteristic velocity, which is taken to be maximum at the centre and zero at the wall (see [14]). Based on the fore-going, the boundary conditions are:

$$u' = 1, v' = 0, T' = 1, C' = 1 \quad \text{at} \quad y' = 0 \tag{5}$$

$$u' = 0, v' = 0, T' = T_w, C' = C_w \quad \text{at} \quad y' = 1 \tag{6}$$

for the upstream/mother channel

$$u' = 0, v' = 0, T' = 0, C' = 0 \quad \text{at} \quad y' = 0 \tag{7}$$

$$u' = 0, v' = 0, T' = \gamma_1 T_w, \quad C' = \gamma_2 C_w, \ \gamma_1 < 1, \ \gamma_2 < 1 \ \text{at} \ y' = \alpha x' \tag{8}$$

for the downstream/daughter channel

Introducing the following non-dimensional variables:

$$x = \frac{x'}{\ell_c}, \ y = \frac{y'}{\ell_c}, \ u = \frac{u'}{U_o}, \ v = \frac{v'}{U_o}, \ p = \frac{p'}{p_\infty}, \ \rho = \frac{\rho'}{U_o^2}, \ \Theta = \frac{T' - T_\infty}{T_w - T_\infty}, \Phi = \frac{C' - C_\infty}{C_w - C_\infty},$$

$$\upsilon = \frac{\mu}{\rho}, \mathrm{Re} = \frac{\rho U_o \ell_c}{\mu}, Gr = \frac{\rho g \beta_t (T_w - T_\infty)\ \ell_c^2}{\mu U_o} \quad Gc = \frac{\rho g \beta_c (C_w - C_\infty)}{\mu U_o}, \chi^2 = \frac{\ell^2{}_c}{\kappa},$$

$$\delta_1^2 = \frac{k_r^2 \ell_c^2}{D}, \ M^2 = \frac{\sigma_e B_o^2\ \ell_c^2}{\rho \mu \mu_m}, \ N^2 = \frac{C_p \mu}{k_o}, \ Sc = \frac{\mu}{\rho D}, \ \mathrm{Pr} = \frac{\mu}{\rho k_o}$$

into equations (1) - (8),we have

$$\frac{\partial u}{\partial x} + \frac{\partial v}{\partial y} = 0 \tag{10}$$

$$\mathrm{Re}\left(u\frac{\partial u}{\partial x}+v\frac{\partial u}{\partial y}\right)=-\frac{\partial p}{\partial x}+\left(\frac{\partial^2 u}{\partial x^2}+\frac{\partial^2 u}{\partial y^2}\right)+Gr\Theta+Gc\Phi-\chi^2 u-M^2 u \tag{11}$$

$$\mathrm{Re}\left(u\frac{\partial v}{\partial x}+v\frac{\partial v}{\partial y}\right)=-\frac{\partial p}{\partial y}+\left(\frac{\partial^2 v}{\partial x^2}+\frac{\partial^2 v}{\partial y^2}\right) \tag{12}$$

$$\mathrm{Re}\,\mathrm{Pr}\left(u\frac{\partial \Theta}{dx}+v\frac{\partial \Theta}{\partial y}\right)=\left(\frac{\partial^2 \Theta}{dx^2}+\frac{\partial^2 \Theta}{\partial y^2}\right)+N^2\Theta \tag{13}$$

$$\mathrm{Re}\,Sc\left(u\frac{\partial \Phi}{dx}+v\frac{\partial \Phi}{\partial y}\right)=\left(\frac{\partial^2 \Phi}{dx^2}+\frac{\partial^2 \Phi}{\partial y^2}\right)+\delta_1^2\Phi \tag{14}$$

with the boundary conditions

$$u=1,\ v=0,\Theta=1,\Phi=1 \quad \text{at} \quad y=0 \tag{15}$$

$$u=0,v=0,\Theta=\Theta_w,\ \Phi=\Phi_w \quad \text{at} \quad y=1 \tag{16}$$

for the upstream channel

$$u=0,v=0,\Theta=0,\Phi=0 \quad \text{at} \quad y=0 \tag{17}$$

$$u=0,v=0,\ \Theta=\gamma_1\Theta_w,\ \ \Phi=\gamma_2\Phi_w,\ \gamma_1<1,\ \gamma_2<1 \ \text{ at } y=\alpha x \tag{18}$$

for the downstream channel

Introducing the similarity solution:

$$\Psi=(U_o \upsilon\, x)^{1/2} f(\eta),\ \eta=\left(\frac{U_o}{\upsilon x}\right)^{1/2} y \tag{19}$$

with the velocity components represented as

$$u=\frac{\partial \Psi}{\partial y},\ \ v=-\frac{\partial \Psi}{\partial x} \tag{20}$$

into equations (10) - (18), we have the following equivalent equations

$$f''=0 \tag{21}$$

$$f'''+f''-M_1^2 f'+\mathrm{Re}(f'f''+ff'')=-Gr\,\Theta-Gc\,\Phi \tag{22}$$

$$\Theta''+\Theta'+\mathrm{Re}\,\mathrm{Pr}(-f'\Theta'+f\Theta')+N^2\Theta=0 \tag{23}$$

$$\Phi''+\Phi'+ReSc(-f'\Phi'+f\Phi')+\delta_1^2\Phi=0 \tag{24}$$

where $M_1^2=(\chi^2+M^2)$

with the boundary conditions:

$$f=1,\ f'=0,\Theta=1,\Phi=1 \quad \text{at } \eta=0 \tag{25}$$

$$f'=0,\ f=0,\ \Theta=\Theta_w,\ \Phi=\Phi_w \quad \text{at} \quad \eta=1 \tag{26}$$

for the upstream channel

$$f=0,\ f'=0,\Theta=0,\Phi=0 \quad \text{at } \eta=0 \tag{27}$$

$$f'=0,\ f=0,\Theta=\gamma_1\Theta_w,\Phi=\gamma_2\Phi_w,\ \ \gamma_1<1,\gamma_2<1 \quad \text{at } \eta=ax \tag{28}$$

for the downstream channel

Equations (21) - (28) show that the similarity equations are coupled and highly non-linear. Therefore, to minimize the effect of non-linearity on the flow variables we introduce perturbation series solutions of the form

$$h(x,y) = h_o(x,y) + \xi h_1(x,y) + \ldots \tag{29}$$

where $\xi = \frac{1}{\mathrm{Re}} << 1$ is the perturbing parameter. We choose this parameter because, almost at the point of bifurcation, due to a change in the geometrical configuration, the inertial force rises and the momentum increases. The increase in the momentum is associated with a drastic increase in the Reynolds number, indicating a sort of turbulent flow at such a point. In this regard, equations (21) - (28) become:
for the zeroth order:

$$f_o'' = 0 \tag{30}$$

$$f_o''' + f_o'' - M_1^{\,2} f_o' = -Gr\Theta_o - Gc\Phi_o \tag{31}$$

$$\Theta''_o + \Theta'_o + N^2\Theta_o = 0 \tag{32}$$

$$\Phi_o'' + \Phi_o' + \delta^2{}_1\Phi_o = 0 \tag{33}$$

with the boundary conditions

$$f_o = 1,\ f_o' = 0,\ f_o'' = 0, \Theta_o = 1, \Phi_o = 1 \quad \text{at} \quad \eta = 0 \tag{34}$$

$$f_o = 0,\ f_o' = 0,\ f_o'' = 0, \Theta_o = 0, \Phi_o = 0 \quad \text{at} \quad \eta = 1 \tag{35}$$

for the first order:

$$f_1'' = 0 \tag{36}$$

$$f_1''' + f_1'' - M_1^{\,2} f_1' = f_o' f_o'' - f_o f_o'' - Gr\Theta_1 - Gc\Phi_1 \tag{37}$$

$$\Theta_1'' + \Theta_1' + N^2\Theta_1 = \mathrm{Pr}(f_o'\Theta'_o - f_o\Theta'_o) \tag{38}$$

$$\Phi_1'' + \Phi_1' + \delta_1^{\,2}\Phi_1 = Sc(f_o'\Phi_o' - f_o\Phi_o') \tag{39}$$

with the boundary conditions

$$f_1 = 0,\ f_1' = 0, \Theta_1 = 0, \Phi_1 = 0 \quad \text{at} \quad \eta = 0 \tag{40}$$

$$f_1 = 0,\ f_1' = 0, \Theta_1 = \gamma_1\Theta_w, \Phi_1 = \gamma_2\Phi_w,\ \gamma_1 < 1, \gamma_2 < 1 \quad \text{at} \quad \eta = ax \tag{41}$$

The zeroth order equations describe the flow in the upstream channel, while the first order equations describe the flow in the downstream channels. The presence of the zeroth order terms in the first order equations indicates the influence of the upstream on the downstream flow.

The solutions to equations (30) - (35) and (36) - (41) are:

$$\Theta_o(\eta) = \frac{\Theta_w e^{\frac{1}{2}(1-\eta)} \sinh\mu_1\eta}{\sinh\mu_1} + \frac{e^{-\frac{1}{2}(1-\eta)} \sinh\mu_1(1-\eta)}{\sinh\mu_1} \tag{42}$$

$$\Phi_o(\eta) = \frac{\Phi_w e^{\frac{1}{2}(1-\eta)} \sinh\mu_2\eta}{\sinh\mu_2} + \frac{e^{-\frac{1}{2}(1-\eta)} \sinh\mu_2(1-\eta)}{\sinh\mu_2} \tag{43}$$

$$f_o(\eta) = \frac{\left(f_{o(p)}(0)e^{-(\mu 3+\eta/2)} \sinh\mu_3\eta\right)}{\sinh\mu_3} + \frac{\left(f_{o(p)}(1)e^{-1/2(1-\eta)} \sinh\mu_3\eta\right)}{\sinh\mu_3} - f_{o(p)}(0)e^{-(\mu_3+\eta/2)} + f_{o(p)}(\eta) \tag{44}$$

for the upstream region

and

$$\Theta_1(\eta) = \frac{\gamma_1 \Theta_w e^{\frac{1}{2}(\alpha x-\eta)} \sinh \mu_1 \eta}{\sinh(\mu_1 \alpha x)} - \frac{\Theta_{1(p)}(\alpha x) e^{-\frac{1}{2}(\alpha x-\eta)} \sinh \mu_1 \eta}{\sinh(\mu_1 \alpha x)}$$

$$+ \frac{\Theta_{1(p)}(0) e^{-(\mu \alpha x+\eta/2)} \sinh \mu_1 \eta}{\sinh(\mu_1 \alpha x)} - \Theta_{1(p)}(0) e^{-(\alpha x-(\mu_1+1/2)\eta)} + \Theta_{1(p)}(\eta) \quad (45)$$

$$\Phi_1(\eta) = \frac{\gamma_2 \Phi_w e^{\frac{1}{2}(\alpha x-\eta)} \sinh \mu_2 \eta}{\sinh(\mu_2 \alpha x)} + \frac{\Phi_{1(p)}(\alpha x) e^{-\frac{1}{2}(\alpha x-\eta)} \sinh \mu_2 \eta}{\sinh(\mu_2 \alpha x)}$$

$$+ \frac{\Phi_{1(p)}(0) e^{-(\mu \alpha x+\eta/2)} \sinh \mu_2 \eta}{\sinh(\mu_2 \alpha x)} - \Phi_{1(p)}(0) e^{-(\alpha x-(\mu_2+1/2)\eta)} + \Phi_{1(p)}(\eta) \quad (46)$$

$$f_1(\eta) = \frac{f_{1(p)}(0) e^{-(\mu_3 \alpha x+\eta/2)} \sinh \mu_3 \eta}{\sinh \mu_3 \alpha x} + \frac{f_{1(p)}(\alpha x) e^{1/2(\alpha x-\eta)} \sinh \mu_3 \eta}{\sinh(\mu_3 \alpha x)}$$

$$- f_{1(p)}(0) e^{(\alpha x-(\mu_{3+1/2})\eta)} + f_{1(p)}(\eta) \quad (47)$$

for the downstream region

3 RESULTS AND DISCUSSION

Using the following realistic and constant values of γ_1 = 0.6, γ_2 =0.6, Φ_w = 2.0, Θ_w =2.0, Pe_h =0.07, Pe_m =0.07, Re= 400, Gr = 0.1, Gc = 0.1, $\delta_1^2 = 0.2$, N^2 =0.2, $\chi^2 = 0.2$ and varied values of α, Re and M^2, we have the results below.

The purpose of this paper is to investigate the effects of bifurcation angle and magnetic field on the flow. To this end, Figure 2 – Figure 7 illustrate the effects of bifurcation angle, Reynolds number and magnetic field on the transport of water in a stream. The results obtained, show that, for varied values of α, Re and M^2 the transport velocity increases as α and Re increase (see Figure 2 - Figure 4), but decreases in the upstream region as M^2 increases (see Figure 5). Furthermore so, the velocity oscillates and fluctuates in the downstream region as M^2 increases (see Figure 6 and Figure 7).

An increase in the angle of bifurcation narrows down the width of the stream, which in turn increases the inlet pressure in the downstream region. Consequent upon this, the velocity increases (see Figure 2 and Figure 3). This agrees with [8], [9], [10], [11], [12] and [13].

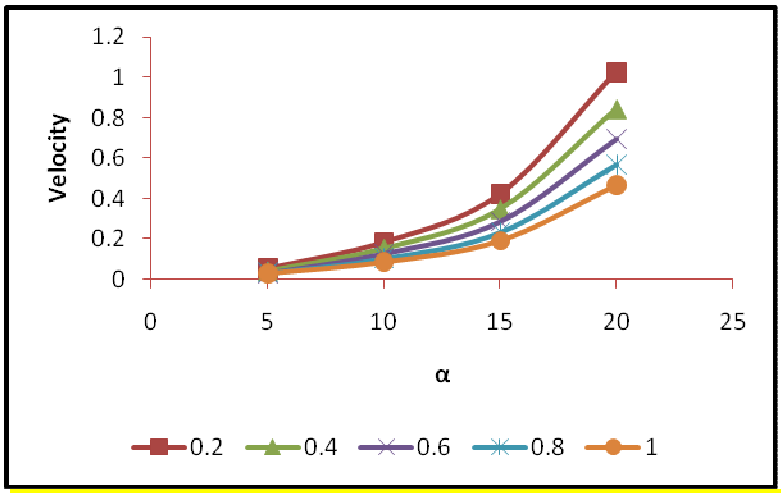

Figure 2 Velocity variations with respect to bifurcation angles (α) in the downstream region

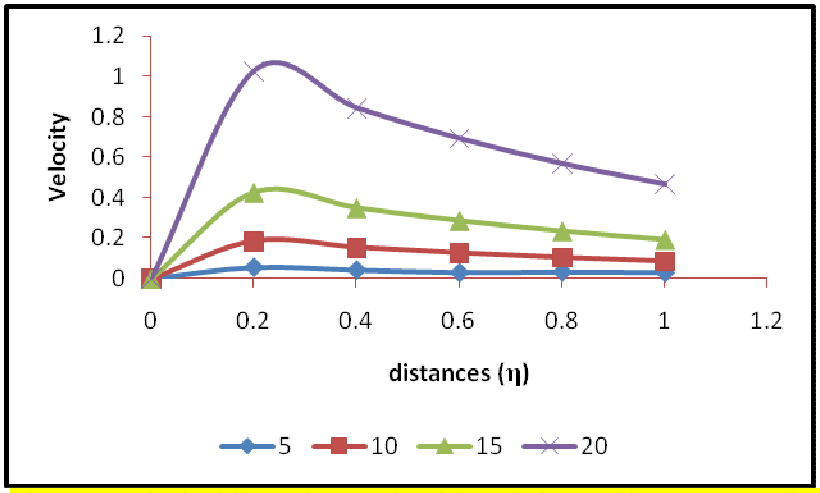

Figure 3 Velocity-bifurcation angles (α) variations with respect to distances (η) in the downstream region.

More so, the flow in the upstream region is laminar and Poiseuille; therefore, its Re is moderate. But, almost at the point of bifurcation or the entry point of the downstream region, the flow exhibits some oscillatory behaviour in the upstream due to a change in geometrical configuration. At this point, the inertial force rises, leading to a drastic increase in the Re. The increase in the Re consequently increases the transport velociy. This accounts for what is seen in Figure 4. As the Re increases the velocity increases and the water rushes into the downstream region with a great force. The flow regains its laminar nature some distance away from the entry region. This result is in perfect agreement with [18].

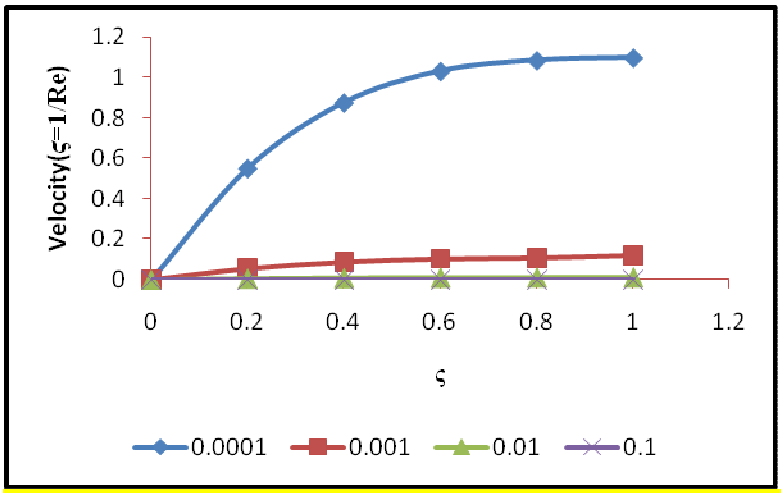

Figure 4 Velocity-Reynolds number (Re) variations with respect to distances (η) in the downstream region.

Similarly, the source rocks in the mountain may be made of metallic oxides and salts. These dissolve in the water to make it alkaline or saline. With this, the water becomes electrolytic, and therefore; exists as charges. The action of the earth magnetic field on the charges produces a mechanical force, the Lorentz force, which gives the flow a new orientation. In particular, the Lorentz force has a freezing impact on the velocity flow structure, thus accounting for what is seen in Figure 5. This result is in consonance with those of [14] and [15]

Also, the oscillatory and fluctuating motion manifested in the form of back-and-forth movement of the water, as seen in Figure 6 and Figure 7, possibly, in addition, may be due to the internal waves developed in the water in the flow process, or may be caused by the interaction between the pressure forces and the gravity forces.

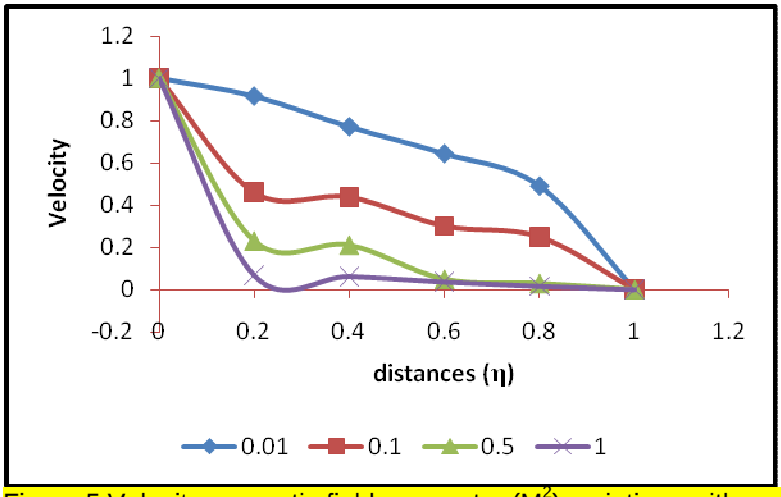

Figure 5 Velocity-magnetic field parameter (M^2) variations with respect to distances (η) in the upstream region

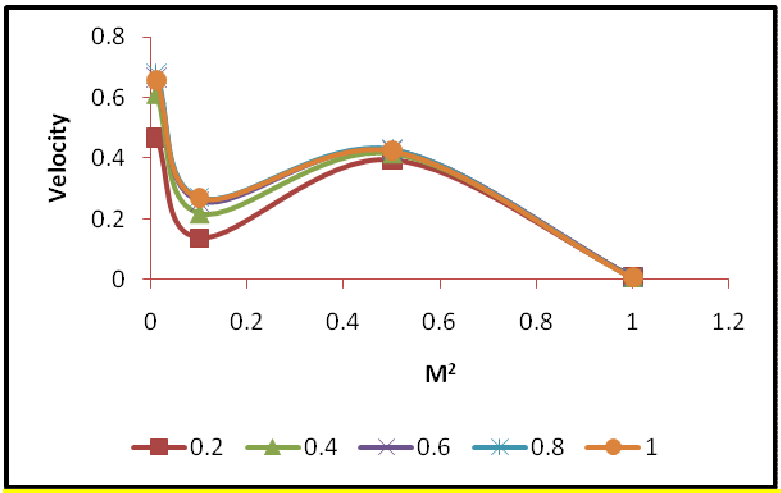

Figure 6 Velocity variations with respect to magnetic field parameter (M^2) in the downstream region

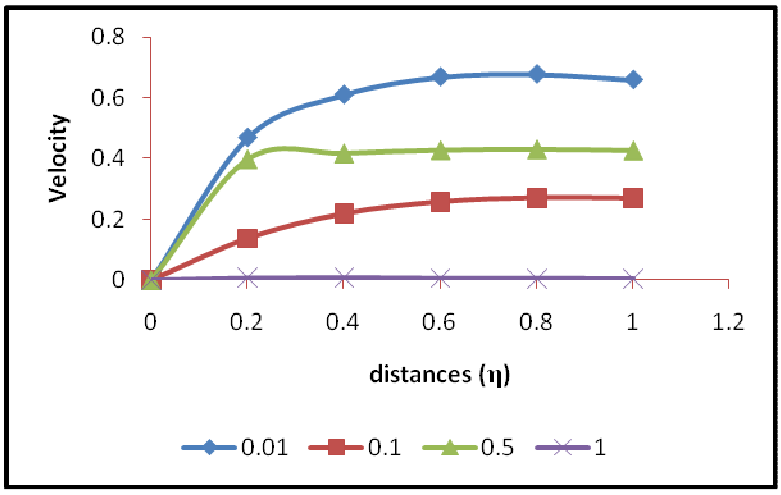

Figure 7 Velocity-magnetic field parameter (M^2) variations with respect to distances (η) in the downstream region

The increase and decrease in velocity, coupled with the oscillatory motion in the downstream have tremendous implications on the flow. The drastic increase in velocity at the inlet of the downstream channel leads to lateral washing away of the embankment, and makes navigation risky; the increase in the velocity enhances the transfer of sediments towards a standing water body ahead of it. On the other hand, the decrease in velocity gives room for early deposition of sediments on the stream bed, and this tends to shallow it up earlier; the oscillatory motion of the fluid at the early stage leads to loss of energy for the flow, and also makes navigation risky.

4 CONCLUSION

The analyses of the flow model show that the velocity increases with bifurcation angle and Reynolds number; magnetic field freezes the motion in the upstream region, and makes it oscillatory in the downstream region. The increase in the velocity enhances the transport of the stream bed loads farther towards the mouths of standing water bodies and saves it from early deposition and shallow-up. The effects of bifurcation angle and Reynolds number tends to cushion the adverse effects of magnetic field on the flow. This study enhances our global understanding of the hydrodynamics of flow in bifurcating streams. It is also relevant to flow in the bifurcating green plants and arteries.

REFERENCES

[1] Makaske Bart. Anastomosing rivers: a review of their classification, origin and sedimentary products. Earth Science Review. 2001; 53:149-96.

[2] Gary Nichols. Sedimentology and Stratigraphy. 2nd Edition. Wiley-Blackwell Publishers; USA; 2009.

[3] Singh VP. Hydrologic systems: volume 1, Rainfall-run-off modeling. Prentice House: Englewood Cliffs, New Jessey; 1988.

[4] Singh VP. Kinematic wave modeling in water resources: surface water hydrology. John Wiley and Sons, New York; 1996.

[5] Hoey T. Temporal variations in bed load transport rate and sediment storage in gravel-bed rivers. Prog. Physical Geography. 1992;16(3): 319–338.

[6] Marusic Galino. A study on the mathematical modeling of water quality in river-type aquatic system. WSEAS Transactions on Fluid Mechanics. 2013; 80–89.

[7] Smith FT. Steady flow through a branching tube. Process Soc. London. 1977; A355:167-187.

[8] Sobey J, Philip Drazin G. Bifurcating two-dimensional flow. J Fluid Mechanics. 1986; 171:263-287.

[9] Smith FT, Jones MA. One-to-few and one-to-many branching tube flow. J Fluid Mechanics. 2000; 423:1–32.

[10] Smith FT, Jones MA. Modeling of multi–branching tube flows: Large flow rates and dual solutions. IMA J Mathematical Medical Biology. 2003; 20:183–204.

[11] Smith FT, Ovenden NC, Frank P, Doorly DJ. What happens to pressure when a fluid enters a side branch. J Fluid Mechanics. 2003; 479: 231–258.

[12] Pittaluga MB, Repetto R, Tubino M. Channel bifurcation in braided rivers: equilibrium configuration and stability. Water Resources Research. 2003; 39(3): 1046–57.

[13] Tadjfar M, Smith FT. Direct simulation and modeling of a 3-dimensional bifurcating tube flow. J Fluid Mechanics. 2004; 519:1-32.

[14] Hogue MM, Anika NN, Alam MM. Numerical analysis of magneto-hydrodynamic fluid flow in a curved duct. International J Scientific and Engineering Research. 2013; 4(7): 607-617.

[15] Hogue MM, Alam MM, Ferdows M, Beg OA. Numerical simulation of Dean number and curvature effects on a magneto-bio-fluid flow through a curved conduit. Process Inst. Mechanical Engineering. 2013; H: 1150-70. DOI: 10.1170/0954411913493844.

[16] Beg OA, Hogue MM, Wahid Uzzaman, Alam MM, Ferdows M. Numerical simulation of magneto-physiological laminar Dean flow. J Medical Biology. 2014; 14:1450047. DOI: http://dx.doi.org/10.1142/S021951941450047.

[17] Hogue MM, Alam MM. A numerical study of MHD flow in a rotating curved pipe with circular cross–section. Open J Fluid Dynamics. 2015; 5:121-127. DOI:10.4236/ojfd.2015:52014

[18] Okuyade WIA, Abbey TM. Oscillatory blood flow in convergent and divergent channels, Part 2: Efects of Reynolds number. British J Mathematics and Computer Science.2016; 15(1):1-14. DOI:10.9734/BJMCS/201623222.

[19] Bestman AR. Global models for the biomechanics of green plants, Part 1, International J Energy Research. 1991; 16:677–84.

APPENDICES

$$f_{o(p)}(\eta) = -\left(\frac{n_3}{n_3\left(n_3^2 - n_2 n_3\right)} - \frac{1}{\left(n_3^2 - n_2 n_3\right)}\right)\left(\frac{GrAe^{\lambda_1\eta}}{\lambda_1} + \frac{GrBe^{\lambda_2\eta}}{\lambda_2} + \frac{GrCe^{m_1\eta}}{m_1} + \frac{GrDe^{m_2\eta}}{m_2}\right)$$

$$+\frac{n_3}{n_3\left(n_3^2 - n_2 n_3\right)}\left(\frac{GrAe^{\lambda_1\eta}}{\left(\lambda_1 - n_2\right)} + \frac{GrBe^{\lambda_2\eta}}{\left(\lambda_2 - n_2\right)} + \frac{GrCe^{m_1\eta}}{\left(m_1 - n_2\right)} + \frac{GrDe^{m_2\eta}}{\left(m_2 - n_2\right)}\right)$$

$$-\frac{1}{n_3\left(n_3^2-n_2n_3\right)}\left(\frac{GrAe^{\lambda_1\eta}}{\left(\lambda_1-n_3\right)}+\frac{GrBe^{\lambda_2\eta}}{\left(\lambda_2-n_3\right)}+\frac{GrCe^{m_1\eta}}{\left(m_1-n_3\right)}+\frac{GrDe^{m_2\eta}}{\left(m_2-n_3\right)}\right)$$

$$\lambda_1=-\frac{1}{2}+\frac{\sqrt{1-4N^2}}{2},\ \lambda_2=-\frac{1}{2}-\frac{\sqrt{1-4N^2}}{2}$$

$$\lambda_1=-\frac{1}{2}+\mu_1,\lambda_2=-\frac{1}{2}-\mu_1,\mu_1=\frac{\sqrt{1-4N^2}}{2}$$

$$m_1=-\frac{1}{2}+\mu_2,m_2=-\frac{1}{2}-\mu_2,\mu_2=\frac{\sqrt{1-4\delta_1^2}}{2}$$

$$n_2=-\frac{1}{2}+\mu_3,n_3=-\frac{1}{2}-\mu_3,\mu_3=\frac{\sqrt{1-4M^2}}{2}$$

$$A=\frac{\Theta_w e^{1/2}-e^{\mu_1}}{\sinh\mu_1},B=\frac{e^{\mu_1}-\Theta_w e^{1/2}}{\sinh\ \mu_1},\ C=\frac{\Phi_w e^{1/2}-e^{\mu_2}}{\sinh\mu_2},D=\frac{e^{\mu_2}-\Phi_w e^{1/2}}{\sinh\mu_2}$$

$$\Theta_{1(p)}(\eta)=\frac{\Pr}{(\lambda_2-\lambda_1)}[\ \ \lambda_1FAe^{(\lambda_1+n_2)\eta}+\lambda_1GAe^{(\lambda_1+n_3)\eta}$$

$$-\left(\frac{n_3}{n_2\left(n_3^2-n_2n_3\right)}-\frac{1}{\left(n_3^2-n_2n_3\right)}\ \right)\left(\begin{array}{l}GrA^2e^{2\lambda_1\eta}+\dfrac{\lambda_1GrABe^{(\lambda_1+\lambda_2)\eta}}{\lambda_2}+\dfrac{\lambda_1GcACe^{(\lambda_1+m_1)\eta}}{m_1}\\+\dfrac{\lambda_1GcADe^{(\lambda_1+m_2)\eta}}{m_2}\end{array}\right)$$

$$+\frac{n_3}{n_2\left(n_3^2-n_2n_3\right)}\left(\frac{\lambda_1GrA^2e^{2\lambda_1\eta}}{\left(\lambda_1-n_2\right)}+\frac{\lambda_1GrABe^{(\lambda_1+\lambda_2)\eta}}{\left(\lambda_2-n_2\right)}+\frac{\lambda_1GcACe^{(\lambda_1+m_1)\eta}}{\left(m_1-n_2\right)}+\frac{\lambda_1GcADe^{(\lambda_1+m_2)\eta}}{\left(m_2-n_2\right)}\right)$$

$$-\frac{1}{\left(n_3^2-n_2n_3\right)}\left(\frac{\lambda_1GrA^2e^{2\lambda_1\eta}}{\left(\lambda_1-n_3\right)}+\frac{\lambda_1GrABe^{(\lambda_1+\lambda_2)\eta}}{\left(\lambda_2-n_3\right)}+\frac{\lambda_1GcACe^{(\lambda_1+m_1)\eta}}{\left(m_1-n_3\right)}+\frac{\lambda_1GcADe^{(\lambda_1+m_2)\eta}}{\left(m_2-n_3\right)}\right)\ ]+\ldots$$

$$\Phi_{1(p)}(\eta)=\frac{Sc}{(m_2-m_1)}[\ \ m_1FCe^{(m_1+n_2)\eta}+m_1GCe^{(m_1+n_3)\eta}$$

$$-\left(\frac{n_3}{n_2\left(n_3^2-n_2n_3\right)}-\frac{1}{\left(n_3^2-n_2n_3\right)}\ \right)\left(\begin{array}{l}\dfrac{m_1GrACe^{(\lambda_1+m_1)\eta}}{\lambda_1}+\dfrac{m_1GrBCe^{(\lambda_2+m_1)\eta}}{\lambda_2}+GcC^2e^{2m_1\eta}\\+\dfrac{m_1GcCDe^{(m_1+m_2)\eta}}{m_2}\end{array}\right)$$

$$+\frac{n_3}{n_2\left(n_3^2-n_2n_3\right)}\left(\frac{m_1GrACe^{(\lambda_1+m_1)\eta}}{\left(\lambda_1-n_2\right)}+\frac{m_1GrBCe^{(\lambda_2+m_1)\eta}}{\left(\lambda_2-n_2\right)}+\frac{m_1GcC^2e^{2m_1\eta}}{\left(m_1-n_2\right)}+\frac{m_1GcCDe^{(m_1+m_2)\eta}}{\left(m_2-n_2\right)}\right)$$

$$-\frac{1}{\left(n_3^2-n_2n_3\right)}\left(\frac{m_1GrACe^{(\lambda_1+m_1)\eta}}{\left(\lambda_1-n_3\right)}+\frac{m_1GrBCe^{(\lambda_2+m_1)\eta}}{\left(\lambda_2-n_3\right)}+\frac{m_1GcC^2e^{2m_1\eta}}{\left(m_1-n_3\right)}+\frac{m_1GcCDe^{(m_1+m_2)\eta}}{\left(m_2-n_3\right)}\right)\ ]+\ldots$$

$$-Gr\ \left\{\frac{\mathrm{J}_1e^{n_1\eta}}{n_2}+\frac{J_2e^{n_2\eta}}{n_2}\ +\frac{\mathrm{Pr}}{\left(\lambda_2-\lambda_1\right)}\left[\frac{\lambda_1FAe^{(\lambda_1+n_2)\eta}}{\left(\lambda_1+n_2\right)}+\frac{\lambda_1GAe^{(\lambda_1+n_3)\eta}}{\left(\lambda_1+n_3\right)}\right.\right.$$

$$-\left(\frac{n_3}{\left(n_3^2-n_2n_3\right)}-\frac{1}{\left(n_3^2-n_2n_3\right)}\right)\left(\frac{GrA^2e^{2\lambda_1\eta}}{2}+\frac{GrBAe^{(\lambda_1+\lambda_2)\eta}}{\left(\lambda_1+\lambda_2\right)}+\frac{\lambda_1GcCAe^{(\lambda_1+m_1)\eta}}{\left(\lambda_1+m_1\right)m_1}+\frac{\lambda_1GcDAe^{(\lambda_1+m_2)\eta}}{\left(\lambda_1+m_2\right)m_2}\right)$$

$$+\frac{n_3}{n_2\left(n_3^2-n_2n_3\right)}\left(\frac{GrA^2e^{2\lambda_1\eta}}{2\left(\lambda_1-n_2\right)}+\frac{\lambda_1GrBAe^{(\lambda_1+\lambda_2)\eta}}{\left(\lambda_2-n_2\right)\left(\lambda_1+\lambda_2\right)}+\frac{\lambda_1GcCAe^{(\lambda_1+m_1)\eta}}{\left(m_1-n_2\right)\left(\lambda_1+m_1\right)}+\frac{\lambda_1GcDAe^{(\lambda_1+m_2)\eta}}{\left(m_2-n_2\right)\left(\lambda_1+m_2\right)}\right)$$

$$-\frac{1}{\left(n_3^2-n_2n_3\right)}\left(\frac{GrA^2e^{2\lambda_1\eta}}{2\left(\lambda_1-n_3\right)}+\frac{\lambda_1GrBAe^{(\lambda_1+\lambda_2)\eta}}{\left(\lambda_2-n_3\right)\left(\lambda_1+\lambda_2\right)}+\frac{\lambda_1GcCAe^{(\lambda_1+m_1)\eta}}{\left(m_1-n_3\right)\left(\lambda_1+m_1\right)}+\frac{\lambda_1GcDAe^{(\lambda_1+m_2)\eta}}{\left(m_2-n_3\right)\left(\lambda_1+m_2\right)}\right)\ ]+\ldots\}$$

$$-\left(\frac{n_3}{n_2\left(n_3^2-n_2n_3\right)}-\frac{1}{\left(n_3^2-n_2n_3\right)}\ \right)\left(\frac{GrAe^{\lambda_1\eta}}{\lambda_1}+\frac{GrBe^{\lambda_2\eta}}{\lambda_2}+\frac{GcCe^{m_1\eta}}{m_1}+\frac{GcDe^{m_2\eta}}{m_2}\right)$$

$$+\frac{n_3}{n_2\left(n_3^2-n_2n_3\right)}\left(\frac{GrAe^{\lambda_1\eta}}{\left(\lambda_1-n_2\right)}+\frac{GrBe^{\lambda_2\eta}}{\left(\lambda_2-n_2\right)}+\frac{GcCe^{m_1\eta}}{\left(m_1-n_2\right)}+\frac{GcDe^{m_2\eta}}{\left(m_2-n_2\right)}\right)$$

$$-\frac{1}{\left(n_3^2-n_2n_3\right)}\left(\frac{GrAe^{\lambda_1\eta}}{\left(\lambda_1-n_3\right)}+\frac{GrBe^{\lambda_2\eta}}{\left(\lambda_2-n_3\right)}+\frac{GcCe^{m_1\eta}}{\left(m_1-n_3\right)}+\frac{GcDe^{m_2\eta}}{\left(m_2-n_3\right)}\right)\ ]+\ldots$$

$$-\left(\frac{n_3}{\left(n_3^2-n_2n_3\right)}-\frac{1}{\left(n_3^2-n_2n_3\right)}\right)\left(\frac{GrA^2e^{2\lambda_1\eta}}{2}+\frac{GrBAe^{(\lambda_1+\lambda_2)\eta}}{(\lambda_1+\lambda_2)}+\frac{\lambda_1GcCAe^{(\lambda_1+m_1)\eta}}{(\lambda_1+m_1)m_1}+\frac{\lambda_1GcDAe^{(\lambda_1+m_2)\eta}}{(\lambda_1+m_2)m_2}\right)$$

$$+\frac{n_3}{n_2\left(n_3^2-n_2n_3\right)}\left(\frac{GrA^2e^{2\lambda_1\eta}}{2(\lambda_1-n_2)}+\frac{\lambda_1GrBAe^{(\lambda_1+\lambda_2)\eta}}{(\lambda_2-n_2)(\lambda_1+\lambda_2)}+\frac{\lambda_1GcCAe^{(\lambda_1+m_1)\eta}}{(m_1-n_2)(\lambda_1+m_1)}+\frac{\lambda_1GcDAe^{(\lambda_1+m_2)\eta}}{(m_2-n_2)(\lambda_1+m_2)}\right)$$

$$-\frac{1}{\left(n_3^2-n_2n_3\right)}\left(\frac{GrA^2e^{2\lambda_1\eta}}{2(\lambda_1-n_3)}+\frac{\lambda_1GrBAe^{(\lambda_1+\lambda_2)\eta}}{(\lambda_2-n_3)(\lambda_1+\lambda_2)}+\frac{\lambda_1GcCAe^{(\lambda_1+m_1)\eta}}{(m_1-n_3)(\lambda_1+m_1)}+\frac{\lambda_1GcDAe^{(\lambda_1+m_2)\eta}}{(m_2-n_3)(\lambda_1+m_2)}\right)\ ]$$

$$+\ldots\quad -Gc\ \left\{\frac{\mathrm{R}_1e^{m_1\eta}}{m_1}+\frac{\mathrm{R}_2e^{m_2\eta}}{m_2}\ +\frac{Sc}{(m_2-m_1)}\left[\frac{m_1FCe^{(m_1+n_2)\eta}}{(m_1+n_2)}+\frac{m_1GCe^{(m_1+n_3)\eta}}{(m_1+n_3)}\right.\right.$$

$$\left(\frac{n_3}{n_2\left(n_3^2-n_2n_3\right)}-\frac{1}{\left(n_3^2-n_2n_3\right)}\right)\left(\frac{m_1GrACe^{\left(m_1+\lambda_1\right)\eta}}{\lambda_1\left(m_1+\lambda_1\right)}+\frac{m_1GrBCe^{\left(m_1+\lambda_1\right)\eta}}{\lambda_2\left(m_1+\lambda_1\right)}+\frac{GcC^2e^{2m_1\eta}}{2m_1}+\frac{m_1GcDCe^{\left(m_1+m_2\right)\eta}}{m_2\left(m_1+m_2\right)}\right)$$

$$-\frac{n_3}{n_2\left(n_3^2-n_2n_3\right)}\left(\frac{m_1GrACe^{\left(m_1+\lambda_1\right)\eta}}{\left(\lambda_1-n_2\right)\left(m_1+\lambda_1\right)}+\frac{m_1GrBCe^{\left(m_1+\lambda_2\right)\eta}}{\left(\lambda_2-n_2\right)\left(m_1+\lambda_2\right)}+\frac{GcC^2e^{2m_1\eta}}{\left(m_1-n_2\right)2}+\frac{m_1GcDCe^{\left(m_1+m_2\right)\eta}}{\left(m_2-n_2\right)\left(m_1+m_2\right)}\right)$$

$$-\frac{1}{\left(n_3^2-n_2n_3\right)}\left(\frac{m_1GrACe^{(m_1+\lambda_1)\eta}}{(\lambda_1-n_3)(m_1+\lambda_1)}+\frac{m_1GrBCe^{(m_1+\lambda_2)\eta}}{(\lambda_2-n_3)(m_1+\lambda_2)}+\frac{GcC^2e^{2m_1\eta}}{(m_1-n_3)2}+\frac{m_1GcDCe^{(m_1+m_2)\eta}}{(m_2-n_3)(m_1+m_2)}\right)\ ]+\ldots]\}$$

$$E=0$$

$$F=\frac{\left(\ f_{o(p)}(0)e^{-(\mu_3+1/2)}-f_{o(p)}(1)\right)e^{1/2}}{2\sinh\mu_3},$$

$$G=\frac{-\left(\ f_{o(p)}(0)e^{-(\mu_3+1/2)}-f_{o(p)}(1)\right)e^{1/2}}{2\sinh\mu_3}-f_{o(p)}(0)$$

$$J_1=\frac{e^{\alpha x/2}\left(\gamma_1\Theta_w-\Theta_{1(p)}(\alpha x)+\Theta_{1(p)}(0)e^{-(\mu_1+1/2)\alpha x}\right)}{2\sinh(\mu_1\alpha x)},$$

455

456 $$J_2 = \frac{-e^{\alpha x/2}\left(\gamma_1\Theta_w - \Theta_{1(p)}(\alpha x) + \Theta_{1(p)}(0)e^{-(\mu_1+1/2)\alpha x}\right)}{2\sinh(\mu_1\alpha x)} - \Theta_{1(p)}(0)$$

457

458 $$R_1 = \frac{e^{\alpha x/2}\left(\gamma_2\Phi_w - \Phi_{1(p)}(\alpha x) + \Phi_{1(p)}(0)e^{-(\mu_2+1/2)\alpha x}\right)}{2\sinh(\mu_2\alpha x)} \quad ,$$

459

460 $$R_2 = \frac{-e^{\alpha x/2}\left(\gamma_2\Phi_w - \Phi_{1(p)}(\alpha x) + \Phi_{1(p)}(0)e^{-(\mu_2+1/2)\alpha x}\right)}{2\sinh(\mu_2\alpha x)} - \Phi_{1(p)}(0)$$

461